PHILOSOPHICAL TRANSACTIONS OF THE ROYAL SOCIETY A

Phil. Trans. R. Soc. A (2006) **364**, 867–884
doi:10.1098/rsta.2006.1743
Published online 22 February 2006

Real-time sea-level gauge observations and operational oceanography

By Baptiste Mourre[1,*], Laurence Crosnier[2] and Christian Le Provost[1]

[1]*LEGOS, 14 avenue Edouard Belin, 31400 Toulouse, France*
[2]*GIP MERCATOR-Ocean, 8-10 rue Hermès, 31526 Ramonville St-Agne, France*

The contribution of tide-gauge data, which provide a unique monitoring of sea-level variability along the coasts of the world ocean, to operational oceanography is discussed in this paper. Two distinct applications that both demonstrate tide-gauge data utility when delivered in real-time are illustrated. The first case details basin-scale operational model validation of the French Mercator operational system applied to the North Atlantic. The accuracy of model outputs in the South Atlantic Bight both at coastal and offshore locations is evaluated using tide-gauge observations. These data enable one to assess the model's nowcasts and forecasts reliability which is needed in order for the model boundary conditions to be delivered to other coastal prediction systems. Such real-time validation is possible as long as data are delivered within a delay of a week. In the second application, tide-gauge data are assimilated in a storm surge model of the North Sea and used to control model trajectories in real-time. Using an advanced assimilation scheme that takes into account the swift evolution of model error statistics, these observations are shown to be very efficient to control model error, provided that they can be assimilated very frequently (i.e. available within a few hours).

Keywords: tide-gauge; sea-level; operational oceanography; model validation; North Atlantic; storm surge modelling

1. Introduction

Sea-level is an important observable parameter of the ocean because it gathers the signature of most of the processes at work at the different temporal and spatial scales. In addition to being observed by satellite since the early 1990s, sea-level has been historically measured by tide-gauges, mainly located along the coasts and around islands. In the context of operational oceanography, which aims at the delivery on a regular basis (typically daily or weekly) of analysis of the state of the ocean and its forecast up to a few days/weeks ahead, these data are likely to provide very valuable support to operational systems. This paper

* Author and address for correspondence: Institut de Ciències del Mar, Physical Oceanography Group, Passeig Marítim 37-49, 08003 Barcelona, Spain (mourre@icm.csic.es).

One contribution of 20 to a Theme Issue 'Sea level science'.

illustrates this ability for two kinds of applications and with a particular emphasis on the need for real-time availability.

The first application concerns the French MERCATOR open ocean forecast system (http://www.mercator-ocean.fr), which is among other goals motivated by the need to provide reliable boundary conditions for coastal prediction systems. Tide-gauge data are not assimilated in the model, partly because data assimilation at the coast still requires further research before it can be used operationally. This relates to the fact that the shape and evolution of model error statistics required for data assimilation experiments have been shown to be more complicated in coastal areas than over the open ocean (Evensen & Drange 1997; Robinson *et al.* 1998; Echevin *et al.* 2000; Auclair *et al.* 2003; Mourre *et al.* 2004). Therefore, coastal tide-gauge measurements are used in this case as independent sea-level data to assess the model's ability to represent sea-level variability at coastal stations (see also Aikman *et al.* 1996; Tokmakian 1996; Smedstad *et al.* 2003; Tokmakian & McClean 2003 for similar experiments with other models). Moreover, a combination of these data with MERCATOR offshore sea-level is performed to demonstrate their utility to estimate the accuracy of the model's meso-scale variability. This experiment is carried out in the southern Gulf Stream region between Cape Canaveral and Cape Hatteras.

The second application extends the work of Mourre *et al.* (2004) on sea-level data assimilation over the European shelf and investigates the contribution of assimilated tide-gauge observations (see also Gerritsen *et al.* 1995; Vested *et al.* 1995 for previous experiments). This case concerns a North Sea storm surge model and the specific model error source under consideration is the bathymetry. Using an ensemble method, Mourre *et al.* (2004) demonstrated that model error statistics due to uncertainties in bathymetry were non-homogeneous, non-isotropic and swiftly evolving depending on the meteorological regime and the associated oceanic processes at work in the region. Therefore, an ensemble Kalman filter assimilation scheme is implemented here to properly take into account the evolution of these complex model error statistics shapes during the assimilation. Multiple twin experiments are then performed to assess the capability of different tide-gauge networks to control this particular type of model error on the North Sea shelf.

2. Model outputs validation: example of the MERCATOR operational system

(*a*) *The MERCATOR system*

The MERCATOR system provides analysis and real-time prediction of three-dimensional ocean conditions in the North Atlantic and the Mediterranean basin at high resolution. The ocean code is based on the 8.1 version of the OPA z-coordinates code (Madec *et al.* 1998), with a rigid lid. The model has a horizontal resolution of 1/15° (5–7 km) and 43 levels in the vertical, with thicknesses ranging from 6 m near the surface to 300 m at depth. It includes a diagnostic ice model, i.e. atmospheric fluxes are set to zero and there is a relaxation to freezing temperature and sea surface salinity in the case of sea ice. Mixed layer dynamics is modelled with a turbulent kinetic energy closure scheme (Blanke & Delecluse 1993). The geographical domain covers the Atlantic and the

Mediterranean basins from 10 to 70° N, with gradual boundary layers in the 65–70° N and 10–15° N latitude bands, where relaxation to the Reynaud *et al.* (1998) seasonal climatology occurs. A relaxation to the seasonal Medatlas (2002) climatology is also applied below 500 m in the Gulf of Cadiz to represent Mediterranean Outflow Water. The bathymetry is taken from the Smith & Sandwell (1997) data base. Momentum and heat forcing are daily updated from the European Center for Medium-Range Weather Forecasts (ECMWF). A weak relaxation to daily (Reynolds & Smith 1994) sea surface temperature and seasonal (Reynaud *et al.* 1998) sea surface salinity is applied at the surface. River runoffs reflect monthly averages and are taken from UNESCO GRDB (1996). The model prognostic variables are the salinity, temperature as well as zonal and meridional velocities and barotropic streamfunction. Open ocean data assimilation is performed in the MERCATOR system. The reduced order optimal interpolation code SOFA (De Mey & Benkiran 2001) is used to assimilate along track altimeter sea-level anomalies (SLA) once a week. The meridional and zonal integration of the pressure gradient on the rigid lid is performed with the addition of a constant pressure computed with the compensation pressure method (Mellor & Wang 1996) on a defined area around the Canaries Islands. This computation leads to the model sea surface height (SSH) diagnostic variable. The mean sea surface height (MSSH) used as a reference during the assimilation procedure is from Rio & Hernandez (2004) based on gravity, altimetry and *in situ* observations in the Atlantic Ocean. The MSSH is subtracted from the model SSH diagnostic variable to give the model SLA. The SLA increments (differences between model and observed SLA) are split into barotropic and baroclinic parts, each of which is then converted into increments for the model prognostic variables (Pinardi *et al.* 1995). The baroclinic part is converted into temperature and salinity increments by applying a lifting–lowering method similar to Cooper & Haines (1996), the barotropic part is converted into barotropic streamfunction increments. Altimeter data assimilation is shut down between the 500 m isobath and the coastline.

(*b*) *Sea-level gauge data*

Tide-gauge SLA time series from the University of Hawaii Sea-Level Center (fast mode data base, Kilonsky *et al.* 1999) are used to validate the MERCATOR-ocean operational forecast system. Twenty hourly time series from 20 coastal stations (figure 1) were collected over an 11 month period from 1 June 2003 to 30 April 2004. An inverse barometer contribution to the sea-level gauge SLA is removed, so that direct comparisons can be made between sea-level gauge and model SLA. The inverse barometer contribution is determined using daily maps from the Carrère & Lyard (2003) MOG2D model (see §3*a* for further details about this model). The tide-gauge hourly values were de-tided using a 3 day Demerliac filter. A 4 day running mean is then applied to MERCATOR and tide-gauge time series.

(*c*) *Comparisons between MERCATOR operational system outputs and sea-level gauge measurements*

Comparisons between model and data over the 11 month period are documented here at three particular coastal stations along the US east coast

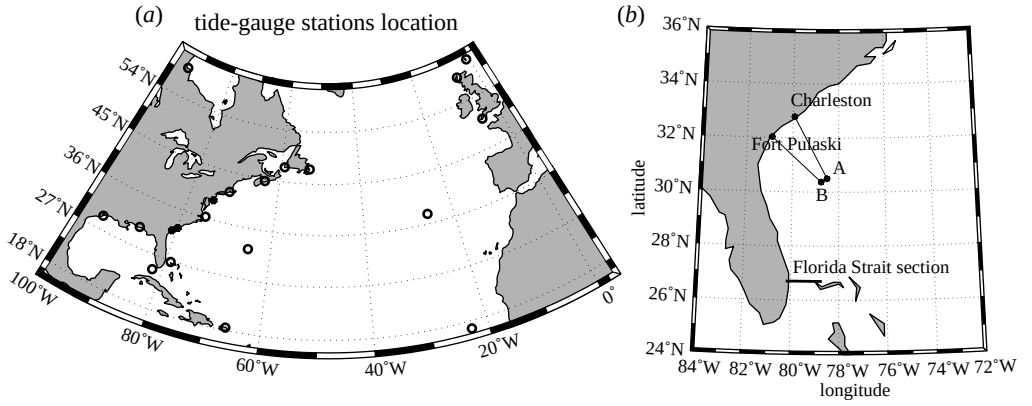

Figure 1. (*a*) Tide-gauge station locations in the North Atlantic are displayed with a round empty circle, except for the Atlantic City, Charleston and Fort Pulaski stations which are displayed as a full black circle. (*b*) Zoom on the location of the Charleston and Fort Pulaski stations as well as the location of the offshore points *A* (30.5° N, 78.5° W) and *B* (30.375° N, 78.75° W) which are chosen in order to capture the entire Gulf Stream transport.

(Atlantic City, Charleston and Fort Pulaski; figure 1*a*). These are the stations with the longest available time series measurements, allowing a proper computation of statistics.

The SLA time series comparison (figure 2) shows that each subtidal event recorded by the tide-gauge time series is also present in the model simulation, although with mismatches. Note also that the smaller amplitude SLA variability during the 2003 summer than in the winter is visible both in the data and in the model. The computation of statistics from these different time series leads to correlation coefficients of 0.51, 0.72 and 0.66 (figure 3*b*), respectively, for the Atlantic City, Charleston and Fort Pulaski stations and r.m.s. differences of 12.3, 9.8 and 11.2 cm (figure 3*c*). Moreover, the ratio between observed and modelled standard deviation (figure 3*a*) shows that the model underestimates the subtidal variability by 25–35% at those three stations locations, as seen in figure 2.

Mismatches between model and data may be due to a lack of resolution in the model associated with a misrepresentation of the smaller scale processes at work and/or a misrepresentation of the coastal bathymetry which results in a Gulf Stream eddy energy too much attenuated on the continental shelf. As it is an open ocean system, the MERCATOR model is not expected to perfectly match coastal sea-level observations. Only a finer regional model resolving realistic smaller scale forcing and dynamics could achieve a perfect accuracy in these areas. We have seen in this paragraph that the model sea-level represents fairly well, although with amplitude and phase mismatches, the subtidal activity of observed tide-gauge along the US east coast. But it is the model behaviour outside of the coastal region that needs to be validated in order to assess whether the MERCATOR system can provide valid boundary conditions for regional models. This is the aim of the following paragraph.

We now investigate the utility of the previously used coastal tide-gauge measurements to assess the accuracy of the MERCATOR model's meso-scale variability. Ezer (2001), using a three-dimensional Atlantic Ocean model forced

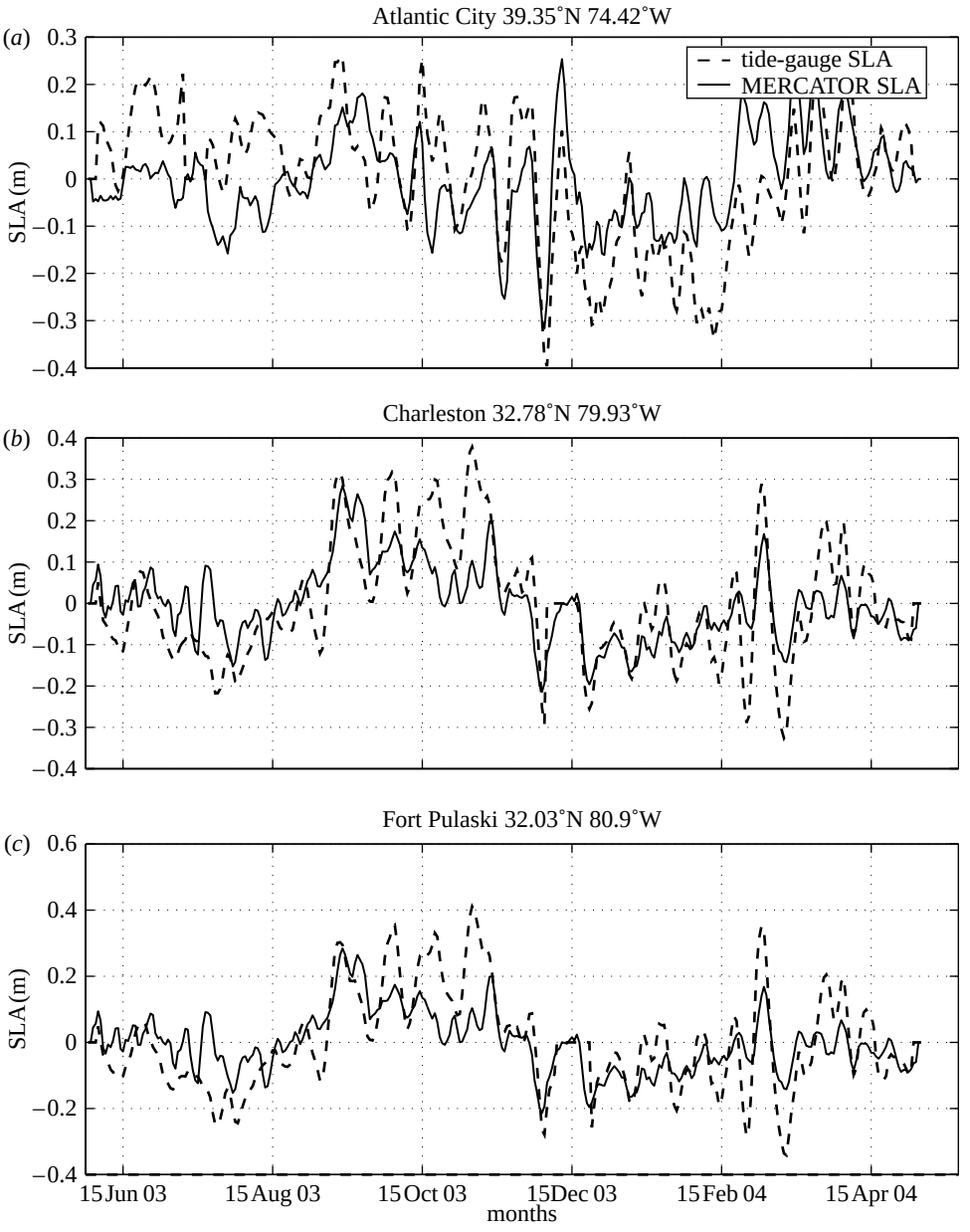

Figure 2. Sea-level anomaly time series at three stations locations (*a*) Atlantic City, (*b*) Charleston and (*c*) Fort Pulaski for the MERCATOR model (solid line) and tide-gauge measurements (dashed line). Mean values have been removed.

by observed surface data, showed that variations in the differences between model offshore and observed coastal sea-level were coherent with variations in the Gulf Stream transport for periods shorter than 1 year and longer than 4–5 years. This suggested that coastal tide-gauge measurements could be used in combination with model offshore sea-level to assess the accuracy of a model

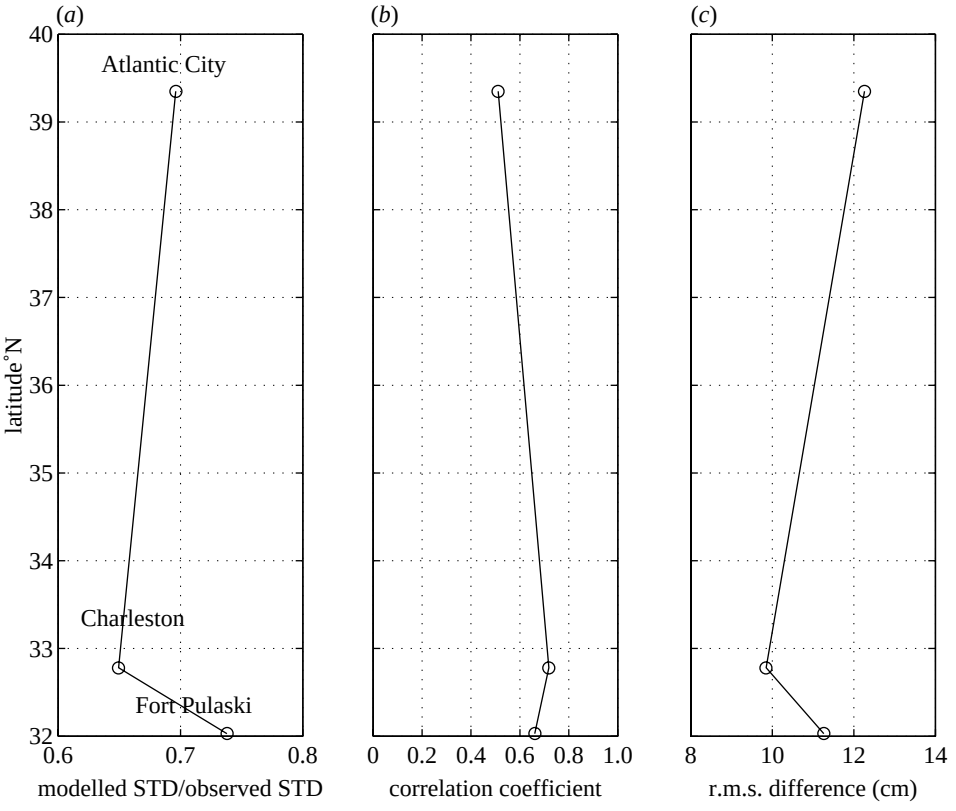

Figure 3. (*a*) Ratio of modelled over observed standard deviation for sea-level anomaly time series at the three stations locations (Atlantic City, Charleston and Fort Pulaski); (*b*) correlation coefficients and (*c*) r.m.s. differences (in centimetres).

meso-scale Gulf Stream variability at periods shorter than a year. Here, we perform an experiment in the southern Gulf Stream region between Cape Canaveral and Cape Hatteras (figure 1*b*), for periods shorter than 1 year, using the Charleston and Fort Pulaski coastal tide-gauge stations as well as offshore model sea-level in comparison to *in situ* Florida current cable transport measurements (M. O. Baringer & C. Meinen, 2002, personal communication, www.aoml.noaa.gov/phod/floridacurrent). The Florida current, with dominant meanders at periods of 12 and 5 days (Johns & Schott 1987) and amplitudes that increase outside of the constraint of the Florida Strait, generates the main form of meso-scale variability between Cape Canaveral and Cape Hatteras. We compute differences between the MERCATOR offshore sea-level and the observed coastal sea-level at the Charleston and Fort Pulaski stations (the Atlantic City station is not considered as it is located north of Cape Hatteras) and compare them to the observed meso-scale variability in the Florida Strait cable measurements. In our computation we use the observed coastal tide-gauge sea-level rather than the model one, the model being less realistic than the tide-gauge in the coastal area as seen in the previous paragraph. As the only non-observed component used in our computation is the offshore model sea-level, we

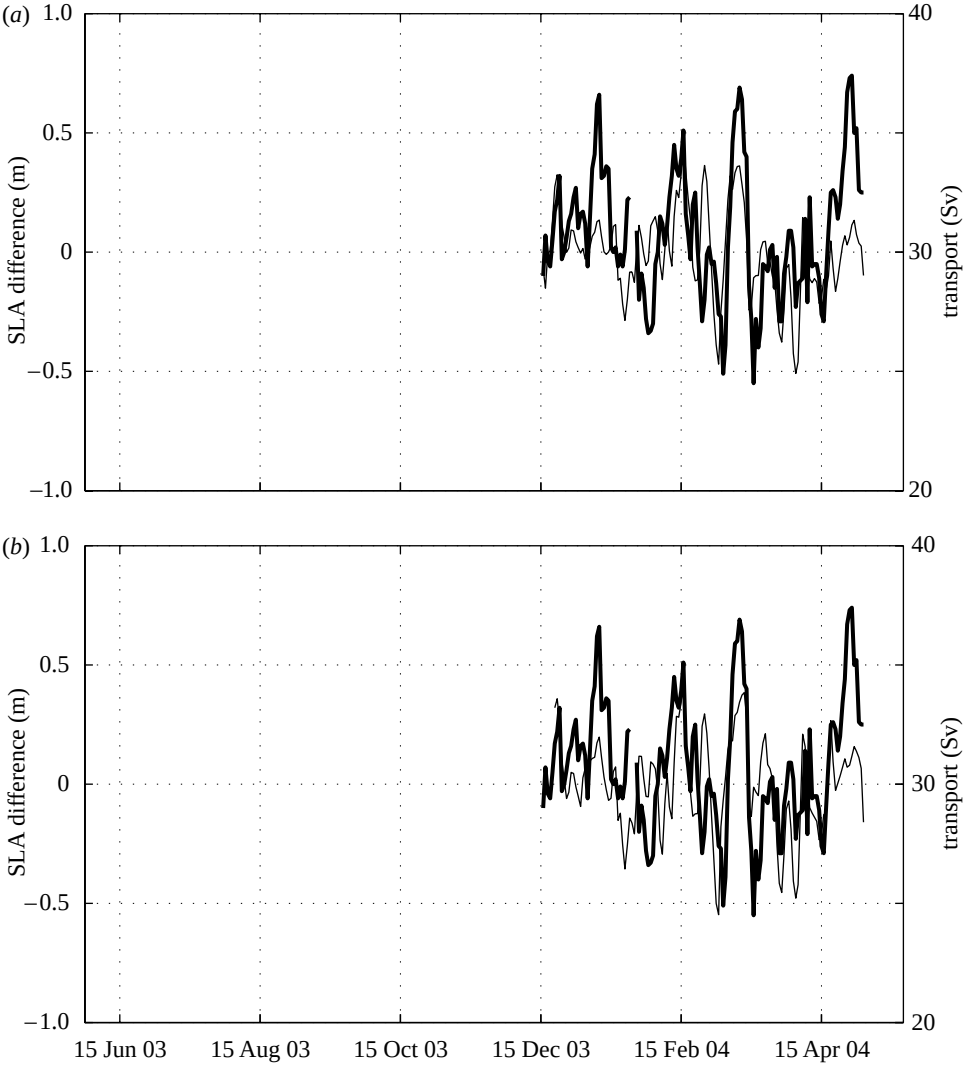

Figure 4. (*a*) Time series of volume transport (Sv) across the Florida–Bahamas section at 27° N from the cable observation (bold solid line, units: Sv, right *Y*-axis) and SLA difference (light solid line, units: m, left *Y*-axis) between the offshore MERCATOR sea-level at point *A* and the Charleston tide-gauge station. (*b*) Same as (*a*) but with SLA difference between the offshore MERCATOR sea-level at point *B* and the Fort Pulaski tide-gauge station. The mean of the sea-level difference is removed.

hope that this experiment will allow us to assess the model offshore sea-level realistic behaviour.

Figure 4 illustrates sea-level differences between the MERCATOR offshore sea-level at point *A* (figure 1*b*) and the observed coastal Charleston tide-gauge data (figure 4*a*, light solid line), as well as sea-level differences between the MERCATOR offshore sea-level at point *B* (figure 1*b*) and the observed coastal Fort Pulaski tide-gauge data (figure 4*b*, light solid line). Locations *A* and *B* are chosen in order to capture the entire transport of the model Gulf Stream. Both

time series of sea-level differences (light solid lines) are coherent with the variability in the observed cable transport (bold solid lines). Moreover, characteristic temporal scales are around a few weeks, denoting the signature of meso-scale activity. The main events of the meso-scale activity seen in the sea-level differences (light solid line) are synchronous with the observed cable transport (bold solid line) meso-scale features. This results from the satellite altimeter data assimilation, which imposes a realistic time pattern to the meso-scale activity in the MERCATOR system. Contrarily, a second simulation without data assimilation does not show meso-scale features synchronous with the cable data (not shown here). The high correlation in the meso-scale variability within Cape Canaveral and Cape Hatteras between the MERCATOR model and the observed Florida current demonstrates with the help of coastal tide-gauge data that the operational system is able to represent a realistic meso-scale activity in this region. Coastal tide-gauge stations are thus useful to validate the MERCATOR system and to show that the meso-scale activity between Cape Canaveral and Cape Hatteras is adequately controlled by the satellite altimetry assimilation. Finer regional models, which require accurate information from the deep open ocean to be applied on their open boundaries, can therefore rely on the MERCATOR outputs to provide proper boundary forcing. Moreover, it is worth noting that due to the temporal scales of sea-level variability in the model (and the time scales of operational requirements), such real-time validation by tide-gauge data is only possible as long as these are delivered within a week or so.

3. Real-time tide-gauge data assimilation for storm surge modelling

(*a*) *Model description and sea-level data assimilation*

The MOG2D model is used in this section to simulate the specific high-frequency response of the ocean to meteorological forcing on the North Sea shelf. MOG2D (D. Greenberg & F. Lyard, 2001, personal communication) is a finite-element, free-surface, barotropic, nonlinear and time-stepping model derived from Lynch & Gray (1979). It solves the classical continuity and momentum equations expressed as a single nonlinear wave equation. The interested reader is referred to Lynch & Gray (1979) and Carrère & Lyard (2003) for a more detailed description of MOG2D. In this paper, the model is forced by atmospheric fields taken from ECMWF analysis, gridded every 1.125° with a 6 h temporal resolution. A tidal velocity background is considered when calculating the dissipation by bottom friction, so that nonlinear interactions between circulations due to tides on the one hand and wind and pressure variations on the other hand are taken into account. An ensemble Kalman filter (Evensen 2003) is then implemented for the assimilation of sea-level data into the model. This sequential data assimilation scheme consists of computing parallel cycles of model integrations and data assimilation steps (called analysis) for each member ($\mathcal{O}(100)$) of a given ensemble. The model stops at observation times and model error covariances required for the analysis are estimated from the ensemble of model states itself, avoiding any linearization when computing the evolution of model error statistics. Following the study of Mourre *et al.* (2004), we focus on the specific model error due to uncertainties in bathymetry. The ensemble of

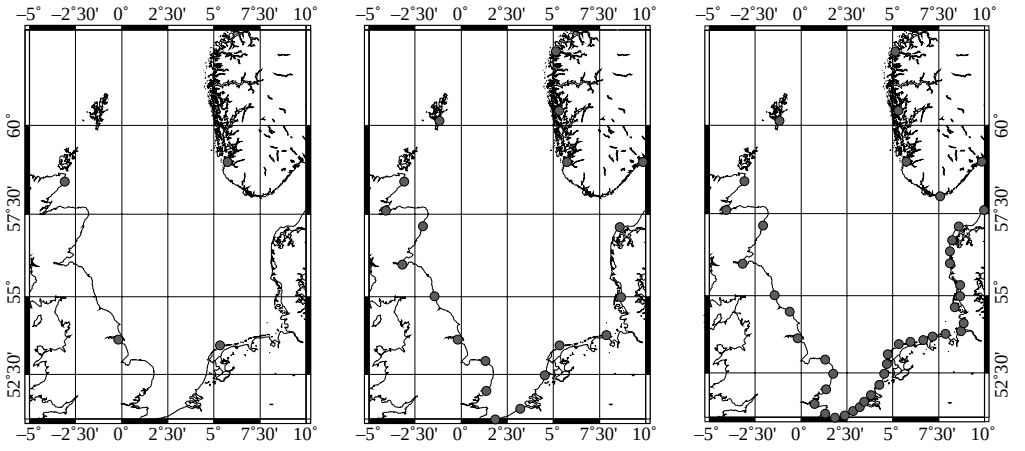

Figure 5. Locations of the stations for the 4, 20 and 44 tide-gauge networks.

model trajectories is provided by running the model over an ensemble of perturbed bathymetric solutions, generated by randomly combining typical mismatches observed between different existing bathymetric databases over the study area. Subsequently, multiple twin experiments are performed to assess the capability of different tide-gauge networks to control this type of model error. The reference model trajectory is computed by running MOG2D over a particular bathymetric solution. Simulated observations at tide-gauge locations are extracted from this simulation, with an additional 1.5 cm r.m.s. Gaussian random noise corresponding to the observational error. Moreover, measurement errors between two different stations are assumed uncorrelated. These simulated observations are then assimilated in each of the 100 perturbed members of the ensemble and the model error reduction by the assimilation is estimated by comparing the evolution of the ensemble spread with assimilation to the one corresponding to the free simulations. Ensemble methods rely on the approximation that: (i) the ensemble mean is the best estimate of the state of the ocean and (ii) the dispersion around this mean provides a representation of the error associated to this estimate (Evensen 2003). Observations at North Sea coastal tide-gauges are assimilated into the model according to four different scenarios: (i) data from four tide-gauges, (ii) data from 20 gauges, (iii) data from 44 gauges (with every location corresponding to an existing station), each assimilated every 6 h and (iv) data from the 20 tide-gauge network assimilated every 12 h, in order to estimate the influence of the assimilation frequency on model error reduction. Tide-gauge locations are represented in figure 5.

(*b*) *Ensemble spread reduction by tide-gauge data assimilation*

(i) *Instantaneous ensemble spread reduction at a given analysis time*

Figure 6 illustrates the reduction of ensemble variances obtained on the North Sea shelf after assimilation of 4, 20 and 44 tide-gauge data on 28 December 1998 at 1 a.m. The distribution of forecast ensemble sea-level variances at this given time (figure 6*a*) is characterized by high values along the Danish coast, at the

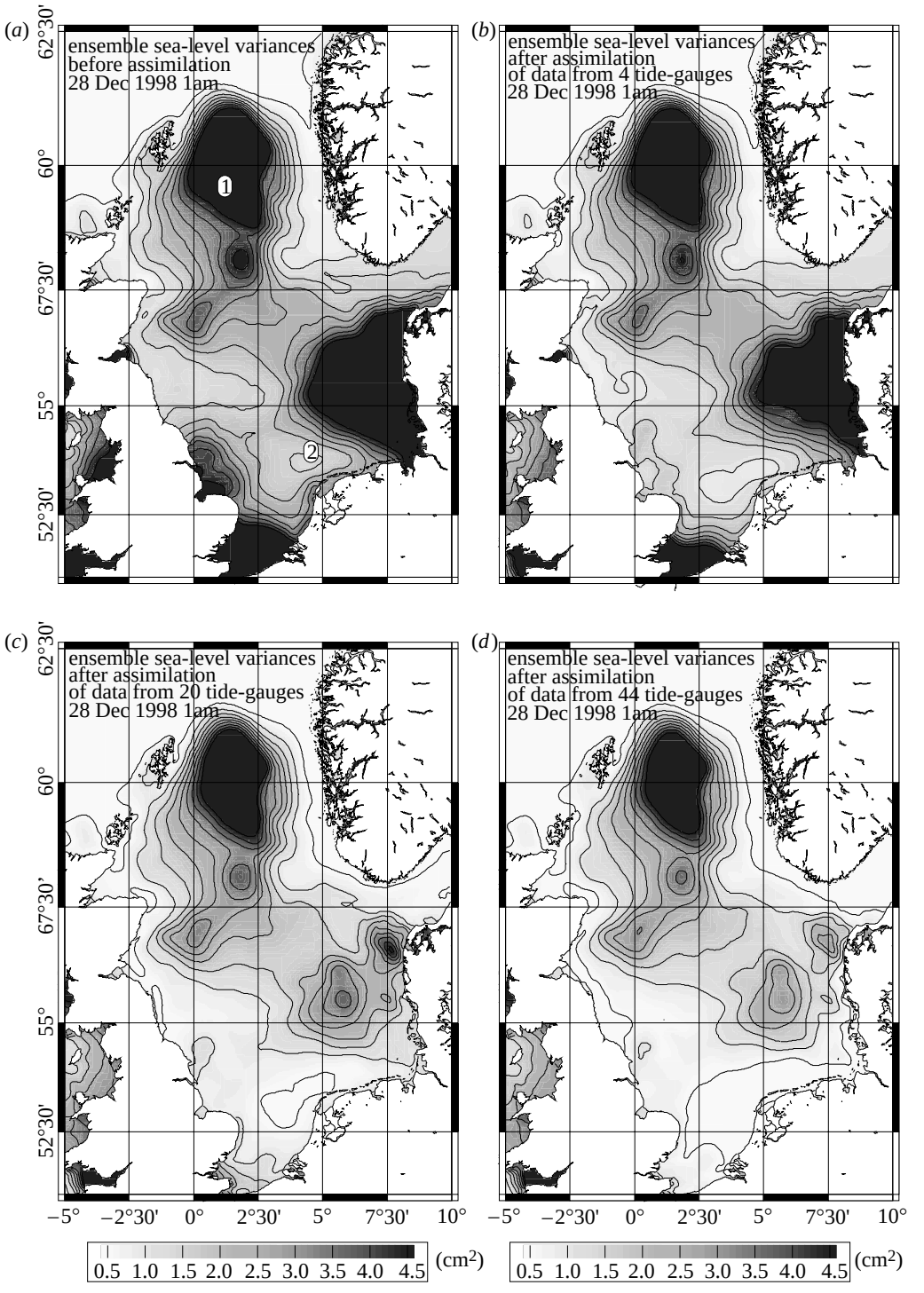

Figure 6. Ensemble sea-level variances before assimilation (*a*) and after assimilation of 4 (*b*), 20 (*c*) and 44 (*d*) tide-gauge data along North Sea coasts on 28 December 1998 at 1 a.m.

English Channel entry, in the Wash (along the southeastern English coast) and finally on the northern shelf between Norway and the Shetland Islands. This last feature reveals that under the current atmospheric circumstances the model is particularly sensitive to bathymetric errors likely to exist at the shelf edge. Moreover, a background level of about 2 cm^2 is present all over the shelf.

The assimilation of data from four tide-gauges (figure 6*b*) only leads to a very weak correction except in the Wash region (the assimilation of the Immingham station is responsible for this). The locations of these four stations are not favourable at the given simulation time. Three of them are located outside regions of high ensemble variances, so that errors in these areas are not likely to be corrected in this configuration. A significant improvement of the correction is obtained after assimilation of data coming from 20 tide-gauges (figure 6*c*), especially along the Danish coast and at the English Channel entry. Some of these are inside the high sea-level variances regions, allowing a significant correction. It is also worth noting that the correction extends relatively far from the coast (around 200 km for the Danish region), illustrating the way the information at the coast is liable to propagate into model sea-level over the shelf for the particular barotropic processes under consideration. The reason is that sea-level error at this given time is empirically well correlated over large areas (more than 100 km) in these high sea-level variances regions. In other words, the domain of influence of a tide-gauge observation in this area (see also Mourre *et al.* 2004) extends more than 100 km away from the station. As the distance between tide-gauges is of the order of 150 km, the assimilation leads to a good control of sea-level model error over the entire 100 km coastal band of the North Sea shelf. Regions of high variances, as well as the background error level, are properly reduced in this area. Nevertheless, the significant spread to the north between Norway and the Shetland Islands remains largely uncorrected, due to the increasing distance from the coast. The 44 tide-gauges assimilation (figure 6*d*) leads to an even better correction, especially off the Danish coast. However, the improvement is not as significant as the multiplication of tide-gauges. The distance between stations is on average shorter than the size of the domain of influence of the observations, so that an important part of the information is redundant in this case for the type of oceanic processes and error source under consideration. These maps illustrate the way the information provided by tide-gauge data can be expected to spatially propagate onto model variables. Yet one should keep in mind that the situation represented here is relative to the particular meteorological circumstances on 28 December 1998 at 1 a.m. and to the resulting oceanic processes at work. Mourre *et al.* (2004) demonstrated that ensemble sea-level variances are very dependent on the atmospheric situation and therefore follow a swift temporal evolution. The time evolution of these ensemble variances has therefore also to be considered.

(ii) *Local ensemble spread reductions over the simulation period*

The two particular locations highlighted on figure 6*a* are now specifically considered. Figure 7 illustrates the reduction of the ensemble spread at point 2 in December 1998 thanks to the assimilation of data from 20 tide-gauges every 6 h. As this location (close to the coast) is inside the domain of influence of the

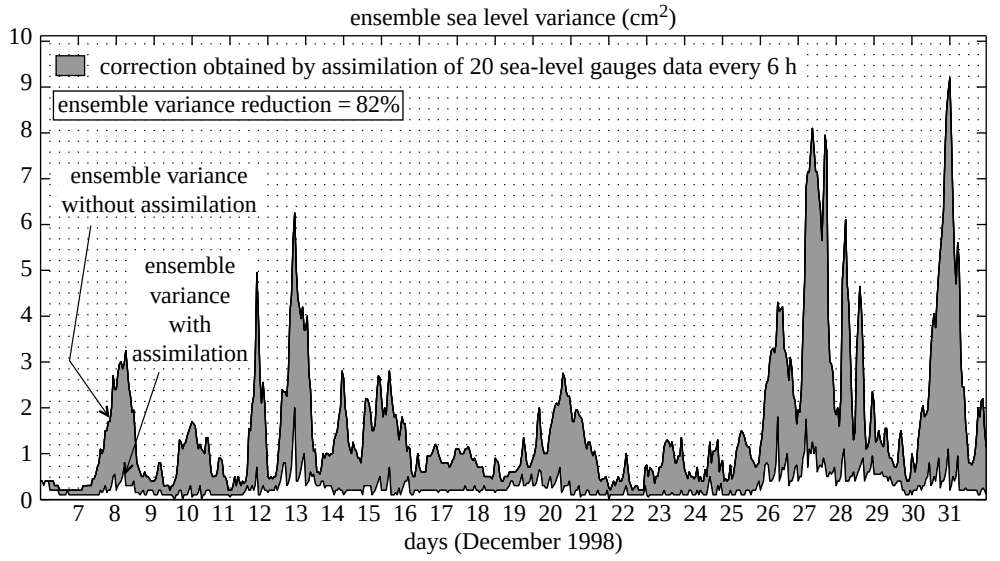

Figure 7. Ensemble sea-level variance evolution at point 2 without assimilation and with assimilation every 6 h of data from 20 tide-gauges.

assimilated Terschelling station, each analysis step (vertical dashed lines) results in a significant reduction of the ensemble sea-level variance. Moreover, the 6 h delay between two analysis steps avoids any significant growth of the dispersion. That way, error peaks, which locally have temporal scales of about 1 day (due to the swift propagation of gravity waves close to the coast) are properly reduced. The global correction over the 25 day period reaches 82% of the ensemble variance without assimilation. Not illustrated here, the other 4 and 44 tide-gauge networks, respectively, allow 66 and 86% of ensemble variance reduction at this location.

The influence of the assimilation frequency is illustrated in figure 8. Data from the 20 tide-gauge network are assimilated every 12 h. In this configuration, the ensemble spread substantially increases between two analysis steps. Some significant values of the ensemble sea-level variance are then reached during periods of high error growth (see peaks around 27 and 31 December). The model error control by tide-gauge assimilation is not as good as the one provided by the 6 h assimilation cycle. The local performance in terms of sea-level model error correction drops from 82 to 68%.

The same kind of diagnostic for the second location farther from the coast is represented in figure 9 for the same 20 tide-gauge network. The correction obtained with a 6 h assimilation of data coming from 20 tide-gauges is locally not as good as for the previous location due to the larger distance to the coast. The ensemble variance is only reduced by 34%. Nevertheless, every analysis step results in a small decrease of the variance, so that the global correction is not zero despite the location far from the assimilated stations. Note also that the temporal scales of variations of the ensemble spread are here longer than the ones encountered at the first location closer to the coast (peaks lasting 2–3 days, see Mourre *et al.* 2004 for further details). The assimilation of 4 and 44 tide-gauge

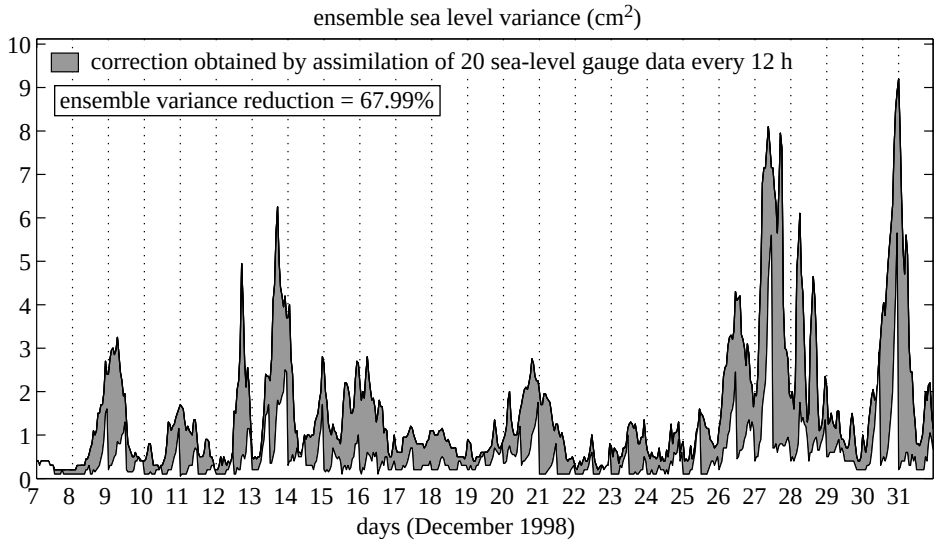

Figure 8. Ensemble sea-level variance evolution at point 2 without assimilation and with assimilation every 12 h of data from 20 tide-gauges.

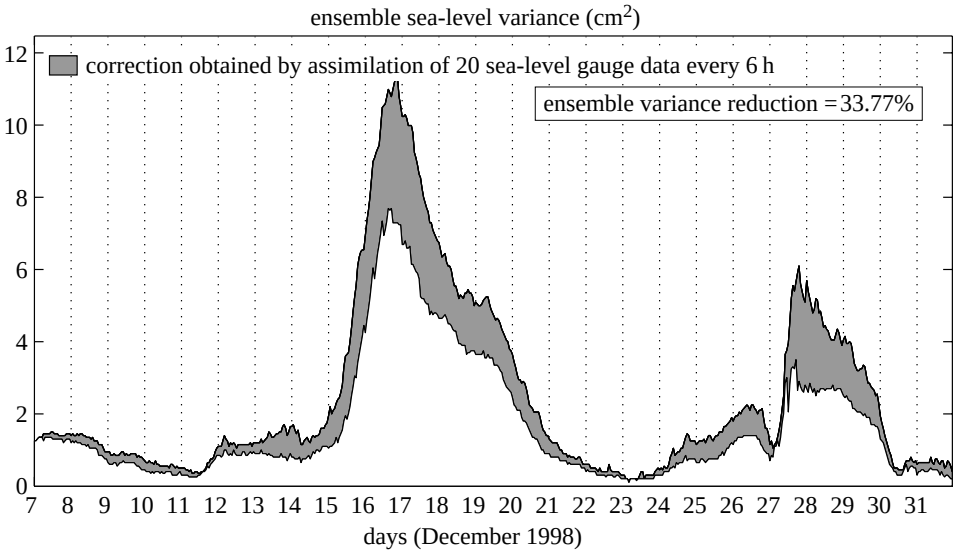

Figure 9. Ensemble sea-level variance evolution at point 1 without assimilation and with assimilation every 6 h of data from 20 tide-gauges.

data locally leads to global corrections, respectively around 11 and 40%. The weak reduction of the dispersion at every analysis step globally results in a significant reduction of ensemble sea-level variances when assimilating a great number of tide-gauge data.

These two particular locations show two different types of model error control likely to be obtained over a given period by assimilation of tide-gauge data over the broad North Sea shelf. In particular, the swift evolution of ensemble

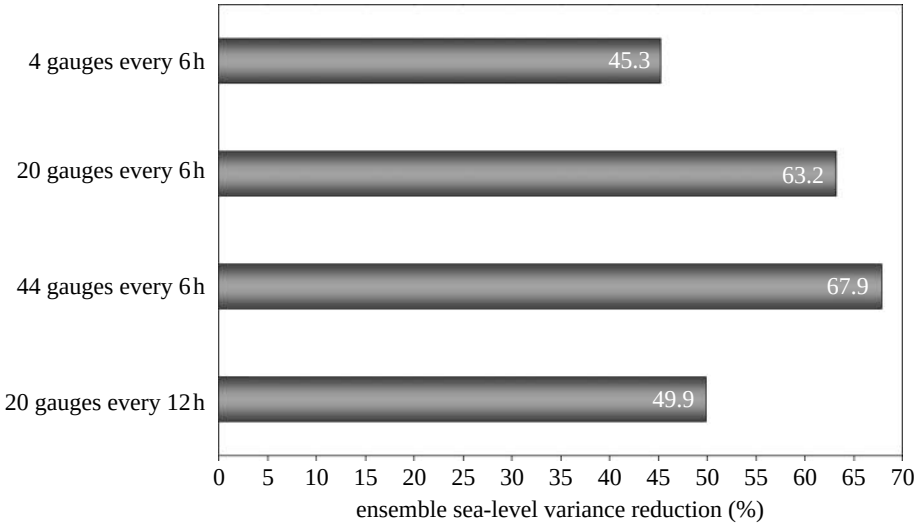

Figure 10. Histogram synthesizing the space–time global performance of the different observing scenarios, in terms of ensemble sea-level variance reduction over the North Sea for a 25 day period in December 1998.

variances next to the coast illustrates the need for fast data delivery, since the error is able to reach significant values within only a few hours. However, this diagnostic is clearly dependent both on the location inside or outside the domain of influence of the considered tide-gauges and on the temporal scales of variations of the associated sea-level error. A more statistical diagnostic is obtained in the following section by considering the global space–time integrated reduction of the ensemble spread.

(iii) *Global space–time integrated performance*

Sea-level. The mean reduction of ensemble variances is calculated over the entire North Sea for a 25 day period in December 1998. The synthetic performance histogram is plotted on figure 10. The frequent assimilation (every 6 h) of tide-gauge data leads to a significant global reduction of the sea-level model error, even with a small number of stations (four tide-gauges allows a global ensemble variance reduction of about 45%). This is mainly due to the spatial propagation of the information contained in the coastal observations over distances around 100 km into model remote locations for the kind of model error under consideration. The assimilation of 20 and 44 tide-gauges every 6 h results in a very good performance (respectively 63 and 68% of model sea-level variance reduction). Moreover, a less frequent assimilation (every 12 h) for the 20 tide-gauge network leads to a global drop in the correction from 63 to 50%.

Barotropic velocities. The impact of sea-level data on non-observed variables is now briefly considered. The global space–time integrated performances concerning zonal barotropic velocity are illustrated in figure 11. Results concerning meridional velocity are very similar. The correction is much weaker than the one obtained for the sea-level variable, as it relies on empirical correlations between model sea-level at observation points and velocities.

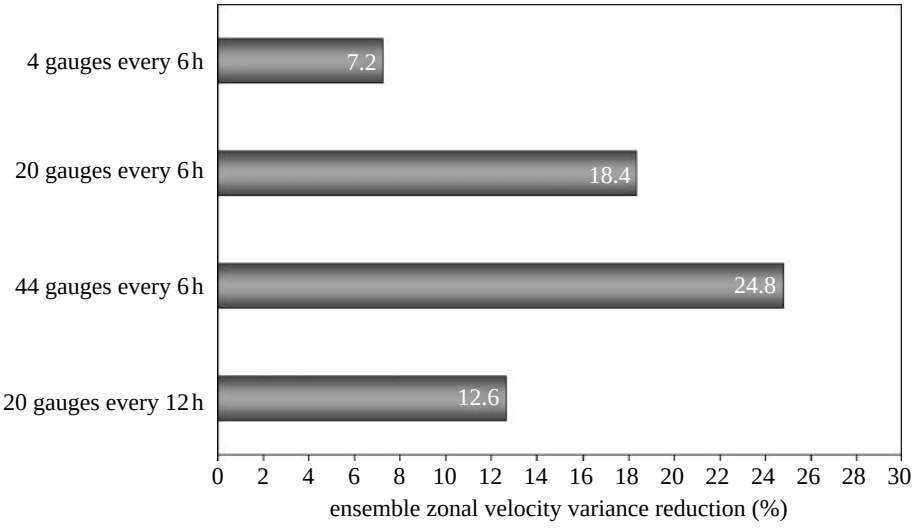

Figure 11. Histogram synthesizing the space–time global performance of the different observing scenarios, in terms of ensemble zonal velocity variance reduction over the North Sea for a 25 day period in December 1998.

Barotropic velocities are more directly controlled by bottom topography (which is the perturbed parameter in this study), so that correlations with sea-level are less significant. Moreover, in the model, the barotropic transport divergence is connected to the sea-level trend through the continuity equation $(\partial h/\partial t) + \nabla\cdot(h\boldsymbol{u}) = 0$. It is therefore likely that the assimilation of sea-level trends instead of instantaneous sea-level data could certainly improve the velocity correction. Nevertheless, the obtained correction is not negligible and reaches more than 20% of the ensemble variance. The differences between the assimilation scenarios are larger since the correction of the smaller scales in the error field benefits higher spatial resolution of the observations.

4. Conclusions

This paper describes two possible uses of real-time sea-level gauge data in the context of operational oceanography. The first one concerns the validation of global or basin-scale forecast systems motivated to provide valid boundary conditions for other coastal prediction systems. Tide-gauge data provide very useful information for real-time checking of model accuracy before it can be used as an operational product. On the one hand, we note that the MERCATOR model coastal sea-level behaviour along the eastern North American coast is in rather good agreement with independent tide-gauge measurements, though the model underestimates by approximately 30% the observed coastal subtidal variability. On the other hand, as it is the model outside of the coastal region that needs to be validated in order to assess whether the model can provide valid boundary conditions for regional models, the offshore sea-level reliability in the South Atlantic Bight region is evaluated. The offshore meso-scale variability between Cape Canaveral and

Cape Hatteras is shown to be realistic in the MERCATOR system using tide-gauge measurements and cable data across the Florida Strait. These model–tide-gauges comparisons make sure that the model sea-level is reliable, thus suggesting that the MERCATOR system outputs can be used as boundary conditions for coastal models. Today, the main limitation for this quasi real-time validation of an operational system by tide-gauge measurements is the real-time delivery of the data, which is not yet sufficient. Requirements for this kind of application are of the order of one week.

Secondly, sea-level gauge measurements have been demonstrated to be very useful when assimilated in a storm surge model for the North Sea. Multiple twin experiments have been carried out to assess the contribution of real-time tide-gauge data for storm surge model error reduction. The global model ensemble variance correction due to the 6 h assimilation of data coming from 20 tide-gauges distributed along North Sea coasts reaches more than 63% for sea-level and 18% concerning zonal velocity. The assimilation of tide-gauge data is then liable to properly control sea-level model error along the coasts, provided that the distance between different stations is of the order of the extension of the domain of influence of the coastal observations relative to the type of error under consideration. This extension is estimated around 100 km in our case, keeping in mind that it strongly evolves with meteorological conditions. Such dense tide-gauge networks presently operate in the North Sea. However, the national diversity in operating these stations and the resulting heterogeneity in the data sampling, quality and archiving complicate the use of such data. The present state of international cooperation is not yet sufficient to meet the needs of models. Projects such as the international permanent service for mean sea-level (PSMSL, http://www.pol.ac.uk/psmsl) or the European ESEAS (European Sea-Level Service, http://www.eseas.org), aiming at collecting and integrating these valuable data into a single easy-to-access source, should considerably improve the situation in the near future. Considering the 20 tide-gauge network, experiments also demonstrated that a decrease of the assimilation frequency from 6 to 12 h led to a loss in performance in sea-level model error reduction from 63 to less than 50%. The swift evolution of model error variances next to the coast makes very frequent assimilation necessary to properly control these errors. This emphasizes the need for real-time delivery of data within 6 h or less.

This paper is dedicated to Christian Le Provost who passed away in February 2004. It is inspired by his presentation given at the Royal Society two weeks before his death. We are grateful to the MERCATOR team in Toulouse for providing its model outputs and to Phillipe Techine and Laurent Roblou from LEGOS, Toulouse, for providing sea-level gauge measurements and inverse barometer data. Part of this work was funded by the Marine Environment and Security for the European Area project (MERSEA) supported by the European Commission under the 6th framework programme. The other part was supported by Centre National Etudes Spatiales (CNES) and Centre National de la Recherche Scientifique (CNRS). The Florida Current cable data are made freely available on the Atlantic Oceanographic and Meteorological Laboratory web page (www.aoml.noaa.gov/phod/floridacurrent) and are funded by the NOAA Office of Climate Observations. Finally, we also wish to thank Philip Woodworth and the three anonymous reviewers for their very useful comments and suggestions that greatly helped to improve the manuscript.

References

Aikman, F., Mellor, G. L., Ezer, T., Sheinin, D., Chen, P., Breaker, L., Bosley, K. & Rao, D. B. 1996 Towards an operational nowcast/forecast system for the US East Coast. In *Modern approaches to data assimilation in ocean modelling* (ed. P. Malanotte-Rizzoli) *Elsevier oceanography series*, 61, pp. 347–376. Amsterdam: Elsevier.

Auclair, F., Marsaleix, P. & De Mey, P. 2003 Space–time structure and dynamics of the forecast error in a coastal circulation model of the Gulf of Lions. *Dyn. Atmos. Oceans* **36**, 309–346. (doi:10.1016/S0377-0265(02)00068-4)

Blanke, B. & Delecluse, P. 1993 Variability of the tropical Atlantic Ocean simulated by a general circulation model with two different mixed layer physics. *J. Phys. Oceanogr.* **23**, 1363–1388. (doi:10.1175/1520-0485(1993)023<1363:VOTTAO>2.0.CO;2)

Carrère, L. & Lyard, F. 2003 Modeling the barotropic response of the global ocean to atmospheric wind and pressure forcing—comparisons with observations. *Geophys. Res. Lett.* **30**, 1275. (doi:10.1029/2002GL016473)

Cooper, M. & Haines, K. 1996 Altimetric assimilation with water property conservation. *J. Geophys. Res.* **101**, 1059–1077. (doi:10.1029/95JC02902)

De Mey, P. & Benkiran, M. 2001 A multivariate reduced-order optimal interpolation method and its application to the Mediterranean basin-scale circulation. In *Ocean forecasting, conceptual basis and applications* (ed. N. Pinardi & J. D. Woods), p. 472. Berlin: Springer.

Echevin, V., De Mey, P. & Evensen, G. 2000 Horizontal and vertical structure of the representer functions for sea surface measurements in a coastal circulation model. *J. Phys. Oceanogr.* **30**, 2627–2635. (doi:10.1175/1520-0485(2000)030<2627:HAVSOT>2.0.CO;2)

Evensen, G. 2003 The ensemble kalman filter: theoretical formulation and practical implementation. *Ocean Dyn.* **53**, 343–367. (doi:10.1007/s10236-003-0036-9)

Evensen, G. & Drange, H. 1997 Data assimilation for coastal zone monitoring and forecasting. In *Operational oceanography: the challenge for European co-operation* (ed. J. H. Stel, H. W. A. Behrens, J. C. Borst, L. J. Droppert & J. v.d.Meulen), pp. 516–522. Amsterdam: Elsevier.

Ezer, T. 2001 Can long-term variability in the Gulf stream transport be inferred from sea level? *Geophys. Res. Lett.* **28**, 1031–1034. (doi:10.1029/2000GL011640)

Gerritsen, H., De Vries, H. & Philippart, M. 1995 The Dutch continental shelf model. In *Quantitative skill assessment for coastal ocean models. Coastal and estuarine studies*, vol. 47 (ed. D. R. Lynch & A. M. Davies). Washington, DC: AGU.

Johns, W. E. & Schott, F. A. 1987 Meandering and transport variations of the Florida current. *J. Phys. Oceanogr.* **17(8)**, 1128–1147. (doi:10.1175/1520-0485(1987)017<1128:MATVOT>2.0.CO;2)

Kilonsky, B., Merrifield, M., Rickards, L. & Woodworth, P. 1999 The WOCE *in situ* sea level program. In *Proc. Conf. on the Ocean observing system for climate*, St Raphael, France, 18–22 October 1999.

Lynch, D. R. & Gray, W. G. 1979 A wave equation model for finite element tidal computation. *Comput. Fluids* **7**, 207–228. (doi:10.1016/0045-7930(79)90037-9)

Madec, G., Delecluse, P., Imbard, M. & Levy, C. 1998 OPA8.1, ocean general circulation model reference manual. *Notes du pole de modelisation IPSL*, vol. 11.

Medatlas 2002 Database, cruise inventory, observed and analysed data of temperature and biochemical parameters (4 CD-ROMS). Medatlas/Medar Group.

Mellor, G. L. & Wang, X. H. 1996 Pressure compensation and the bottom boundary layer. *J. Phys. Oceanogr.* **26**, 2214–2222. (doi:10.1175/1520-0485(1996)026<2214:PCATBB>2.0.CO;2)

Mourre, B., De Mey, P., Lyard, F. & Le Provost, C. 2004 Assimilation of sea level data over continental shelves: an ensemble method for the exploration of model errors due to uncertainties in bathymetry. *Dyn. Atmos. Oceans* **38**, 93–121. (doi:10.1016/j.dynatmoce.2004.09.001)

Pinardi, N., Rosati, A. & Pacanowski, R. C. 1995 The sea surface pressure formulation of rigid lid models. Implications for altimetric data assimilation studies. *J. Mar. Syst.* **6**, 109–119. (doi:10.1016/0924-7963(94)00011-Y)

Reynaud, T., Legrand, P., Mercier, H. & Barnier, B. 1998 A new analysis of hydrographic data in the Atlantic and its application to an inverse modeling study. *Int. WOCE Newslett.* **32**, 29–31.

Reynolds, R. W. & Smith, T. 1994 Improved global sea surface temperature analysis using optimum interpolation. *J. Clim.* **7**, 929–948. (doi:10.1175/1520-0442(1994)007<0929:IGSSTA>2.0.CO;2)

Rio, M.-H. & Hernandez, F. 2004 A mean dynamic topography computed over the world ocean from altimetry, *in-situ* measurements and a geoid model. *J. Geophys. Res.* **109**. (doi:10.1029/2003JC002226) C12032 1-19.

Robinson, A. R., Lermusiaux, P. F. J. & Quincy Sloan III, N. 1998 Data assimilation. In *The sea. The global coastal ocean: processes and methods*, vol. 10, ch. 20 (ed. K. H. Brink & A. R. Robinson). New York: Wiley.

Smedstad, O. M., Hurlburt, H. E., Metzger, E. J., Rhodes, R.., Shriver, J. F., Wallcraft, A. J. & Kara, A. B. 2003 An operational eddy resolving 1/16 degree global ocean nowcast/forecast system. *J. Mar. Syst.* **40-41**, 341–361. (doi:10.1016/S0924-7963(03)00024-1)

Smith, W. H. F. & Sandwell, D. T. 1997 Global sea floor topography from satellite altimetry and ship depth soundings. *Science* **277**, 1956–1962. (doi:10.1126/science.277.5334.1956)

Tokmakian, R. 1996 Comparisons of time series from two global models with tide-gauge data. *Geophys. Res. Lett.* **23**, 3759. (doi:10.1029/96GL03583)

Tokmakian, R. & McClean, J. L. 2003 How realistic is the high-frequency signal of a 0.1 Å resolution ocean model? *J. Geophys. Res.* **108**, 3115. (doi:10.1029/2002JC001446)

UNESCO 1996 Global river discharge database (RivDis v1.0), A contribution to IHP-V Theme 1. Technical documents in hydrology series. Compiled by C. J. Vörösmarty, B. M. Fekete & B. A. Tucker, Vol 0: Introduction, overview and technical notes, Vol I: Africa (198 stations), Vol II: Asia (215 stations), Vol III: Europe (152 stations), Vol IV: North America (251 stations), Vol V: South America (104 stations), Vol VI: Oceania (29 stations).

Vested, H. J., Nielsen, J. W., Jensen, H. R. & Kristensen, K. B. 1995 Skill assessment of an operational hydrodynamic forecast system for the North Sea and Danish belts. In *Quantitative skill assessment for coastal ocean models. Coastal and estuarine studies*, vol. 47 (ed. D. R. Lynch & A. M. Davies), pp. 373–396. Washington, DC: AGU.